ASSESSING BIOMASS YIELD OF KALE (*BRASSICA OLERACEA VAR. ACEPHALA L.*) FIELDS USING MULTI-SPECTRAL AERIAL PHOTOGRAPHY

Jaco Fourie, Armin Werner and Nicolas Dagorn

Lincoln Agritech Ltd, Canterbury, New Zealand
jaco.fourie@lincolnagritech.co.nz

Abstract
Aerial images were taken in June 2014 with a multispectral VIS/NIR camera of the canopy from 14 kale (Brassica oleracea var. acephala L.) fields in Canterbury, New Zealand before this forage was grazed by cows. Images were taken at 716m and at 1,372m flying altitude. Calculating the *Green Normalised Difference Vegetation Index (GNDVI)* from green and NIR channels proved to be the best representation of yield (dry matter) variation from manual biomass cuts in these fields. Several hundreds of individual images covering parts of the fields were semi-automatically stitched to composite images covering full blocks of fields. Highest coefficients of variation (CV) of GNDVI values in a field are linked with low yield averages, often found at vary patchy fields (CVs of 20%). High yielding fields were less patchy and had CVs of less than 8%.

A non-linear calibration curve was derived from the presented data. This functional relationship can explain 70% of the variance of the measured biomass yield data with reflection data of the canopy from these fields. This explaining power does not change when data from aerial images from higher altitudes were analysed. This independency of the preliminary model from height will allow using such an approach with standard high resolution cameras from various platforms (e.g. conventional aircraft, UAV/ RPAS).

Grouping the GNDVI data also allows delineating zones of similar yield levels within the forage fields. Such zoning enables farmers to adapt fertilizer application to the yield expectation of such zones or to manage the feed provision for their grazing cows in a spatial variable way across and between fields. The zones can be used for directing the manual sampling of biomass in cases when farmers deem estimations of biomass yield from aerial imagery to be inaccurate. For all these steps higher resolutions - associated with lower flying altitudes - are necessary.

Introduction
Assessing the dry matter amount from standing biomass on fields is methodologically difficult, as it involves manual sampling and measuring the total biomass as well as the dry matter content. In addition most fields show spatial heterogeneity of their growth conditions and thus varying yield levels within fields. Farmers that grow forage for winter grazing of cattle frequently find that kale-fed cows have been fed less dry matter than the assessed yield, as rated through body scoring. Judson and Edwards (Judson and Edwards 2008) show that 2/3 of herds wintered on kale consumed significantly less than their target feed intake as a result of inaccurate crop allocation. Yield data for paddocks of kale are based on results from manual yield sampling of a small number of test sites and individual field inspections, as this is the current norm (Matthew, et al. 2011). Due to the heterogeneity of growth conditions

within a field, variations in dry matter yield of kale range between 50% - 80%. These errors are caused by difficulties to identify the most representative sites for sampling as well as inaccurate estimation of the areas of similar yield (Pangborn and Gibbs 2011).

Methods are necessary that provide more accurate localizing of representative sites as well as approaches which deliver data that can provide more accurate dry matter yield assessments. The obvious solution is to utilise aerial remote sensing to rapidly and cheaply gather high resolution data on biomass of whole paddocks, as well as for many paddocks. Such sensing platforms can be carried by traditional aircraft, unmanned aircraft systems (UAVs), or via satellite. Several companies in most countries are preparing to provide data for such platforms in agriculture on demand or as a regular service.

The field of remote sensing of characteristics from standing forage is not well developed, due to the internationally rare use of arable forage crops for grazing. We did not find any remote sensing reference covering the forage kale or comparable plant types. This is different to other crops, e.g. fodder beets, as they can be close to growth habits and canopy structure of sugar beets (Hoffmann and Blomberg 2004).

To develop the methodology we investigated kale that was to be grazed in winter (June – August) 2014 on selected fields in Canterbury, New Zealand. Aerial data as well as manual cuts of biomass will be used to establish functional relationships based on reflectance characteristics of the crop canopy.

Data capture and image processing

We captured image data using a multispectral camera that provides 4 separate colour channels namely, red, green, blue and near-infra-red (NIR).The JAI AD-080GE is a multi-spectral CCD camera developed for applications that require simultaneous colour and NIR imaging (JAI 2014) (see Figure 1). It features a single optical path setup whereby a prism is used to split the colour and NIR light onto two separate CCD sensors. This setup is illustrated in Figure 2.

Figure 1: The JAI AD-080GE multispectral camera

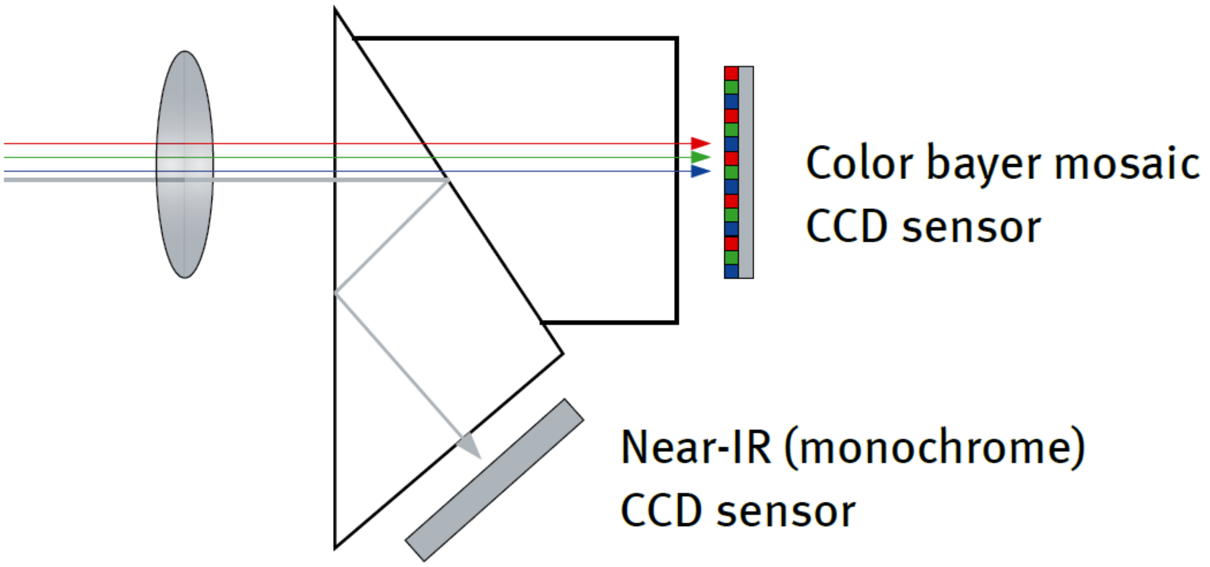

Figure 2: The single optical path setup of the JAI camera

For our aerial surveys we mounted the camera on the floor of a light 4-seat aircraft (Piper Warrior - PA28 161). Our test site was a series of Kale fields near the town of Hororata in southern Canterbury, New Zealand. The total area of the fields we surveyed is approximately 135 ha. The height at which the images were captured was approximately 2350 ft (716 m). The survey area is shown in Figure 3 as a stitched composite of all the images captured.

Figure 3: The survey area covers several fields with a total area of approximately 135 ha.

The 4 channels of image are combined to from a vegetation index called the green normalised difference vegetation index (GNDVI) (Gitelson and Merzlyak 1994). This vegetation index has been found to be particularly suited for prediction of yield in winter wheat (Moges, et al. 2005). The GNDVI uses the green and NIR channels to form a crop vigour index defined as

$$GNDVI = \frac{NIR - G}{NIR + G}$$

By applying this equation to every pixel in the original image we can convert the normal colour image into a GNDVI image where the brightness of each pixel represents the index value at that location. An example of a normal colour image compared with the GNDVI image of the same area is shown in Figure 4.

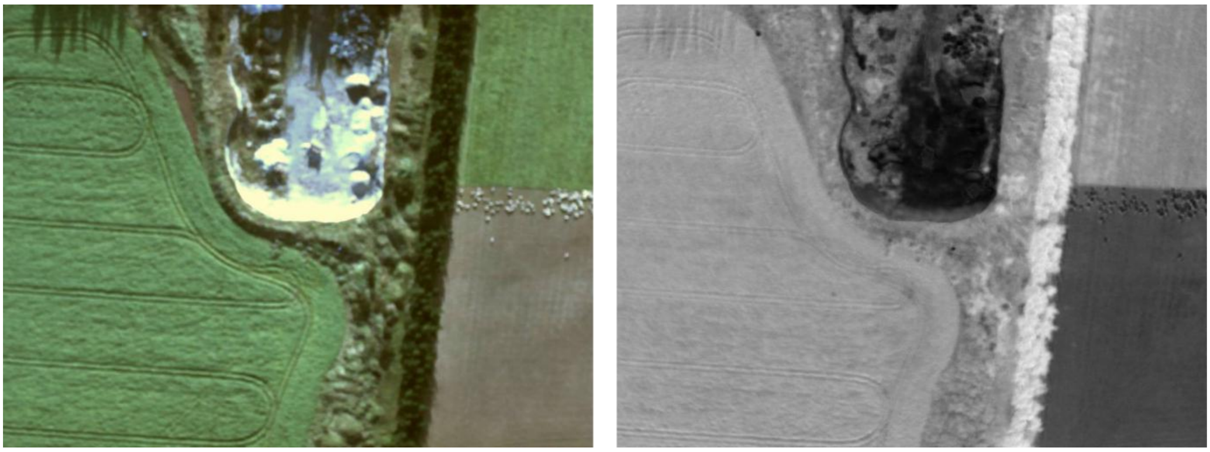

Figure 4: The image on the left is normal colour while the one on the right is a GNDVI image of the same area.

Notice how the vegetation in Figure 4 shows up as bright areas in the GNDVI image while non-vegetation areas are dark.

The GNDVI images are combined into a composite image of the entire area called the GNDVI mosaic which is similar to the example of Figure 3. The mosaic is made by using specialised software that combines images that contain matching features and then stitches them together into one large composite image by lining up the features that match.

Results

Our aim was to show that a model can be constructed based on GNDVI that would allow us to predict kale yield using the multi-spectral images from our aerial survey. This would be a result similar to that reported by (Moges, et al. 2005) that was based on winter wheat yields.

In Table 1 the yields and average GNDVI scores from 14 fields in the survey area are given. Not all the fields in the survey area were included in the study as accurate yield data were not available for all fields. Also included in the table is the standard deviation of the GNDVI values which gives an indication of the variation within the field. The size of this variation in relation to the average GNDVI, called the coefficient of variation, is expressed as a percentage in the final column of the table.

Yield (t/ha)	GNDVI	δ	$\frac{d}{GNDVI}$ (%)
4.3	0.55	0.04	8.07
7.3	0.64	0.03	5.24
5.7	0.62	0.03	5.59
5.5	0.59	0.04	6.10
4.6	0.47	0.09	19.18
7.1	0.59	0.04	7.06
8.6	0.60	0.05	7.64
7.8	0.66	0.04	5.39
6.9	0.72	0.04	5.80
3.6	0.38	0.08	20.26
7.9	0.70	0.03	4.21
7.5	0.65	0.03	4.00
6.5	0.60	0.03	5.69
7.9	0.67	0.03	3.92

Table 1: Yields and GNDVI scores from 14 fields

The results from Table 1 can be used to make a predictive model of yield based on the average GNDVI score. By fitting a logarithmic curve to the data as shown in Figure 5 we create a yield model that has a R^2 coefficient of determination of 0.697.

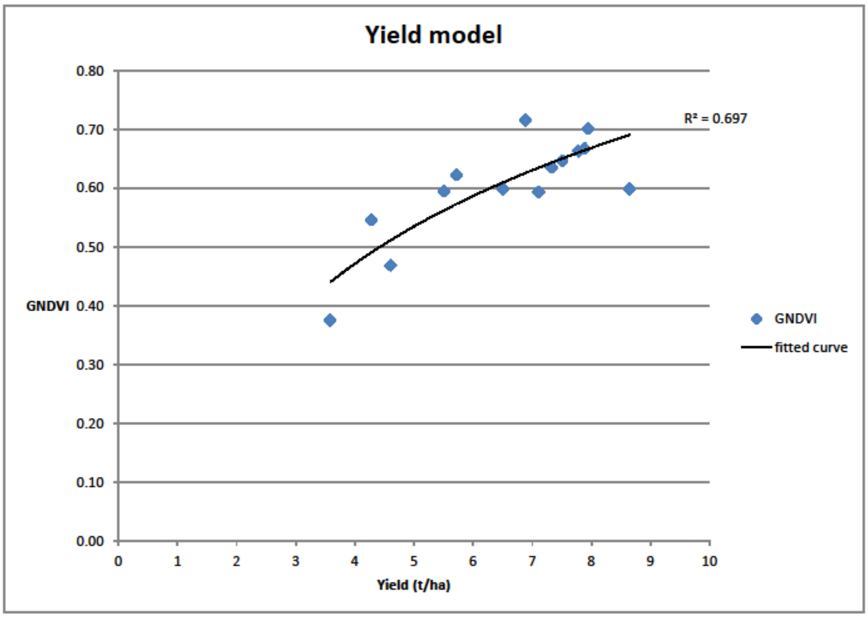

Figure 5: This yield model is based on the data from Table 1 and has a R^2 value of 0.697.

In Figure 6 the fields that were considered in this study are highlighted. Based on the GNDVI score and the yield prediction model we grouped the fields into three categories. The fields labelled as LOW are those the model predicts will have low yields and in a similar way MED and HIGH are those the model predicts will have average and better than average yields. The numbers on the fields indicate the actual recorded yield in t/ha and show the relationship between the predicted yield categories and the actual yield.

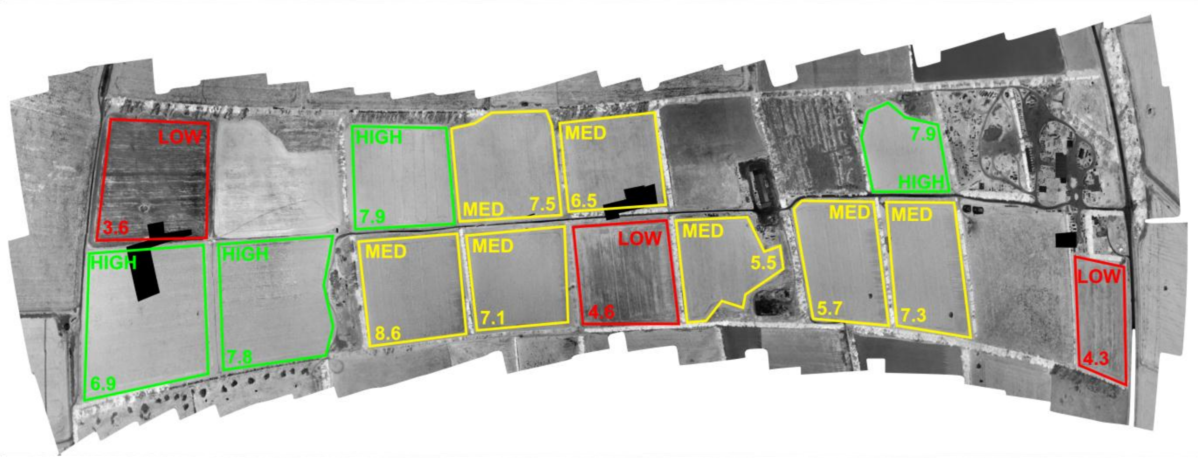

Figure 6: This GNDVI mosaic highlights the fields included in the survey. The fields are classified by GNDVI score into three categories based on the predicted yield. The numbers indicate the actual recorded yield in t/ha.

We repeated the survey flight at a much higher altitude of 4500 ft (1371.6 m) in order to determine the effect the reduced image resolution would have on the accuracy of the GNDVI averages. The results from this flight compared with the original lower altitude flight are shown in Figure 7. The GNDVI (low alt) dataset is the same one seen in Figure 5 and we notice that the same trend is visible in the new GNDVI (high alt) dataset. These results indicate that at this scale altitude makes little difference to the construction of the yield model.

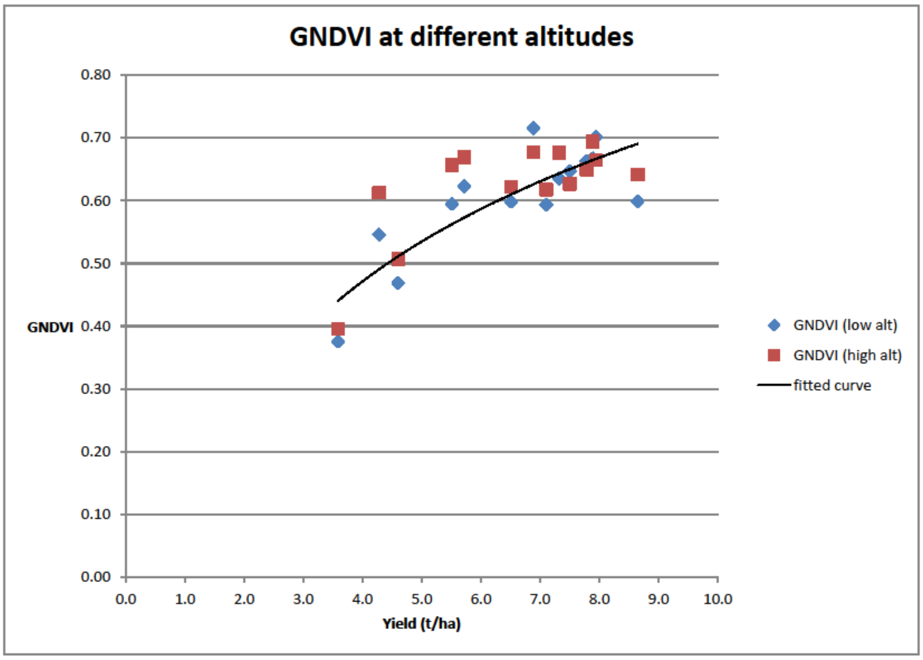

Figure 7: Average GNDVI values from the same survey area but captured at different altitudes are compared in this graph.

Our dataset only deals with yield values on a per field basis but the real value of this approach is in identifying those areas of the field where one can expect higher or lower than expected yields. Instead of comparing yields and average GNDVI scores between fields we can use the model to predict different yield zones in the field. This will be useful not only in highlighting the variability of a field but can also point a farm manger to specific areas in a field that need to be investigated further.

In the example of Figure 8 we chose one of the fields from the survey of Figure 6 that had an average yield predicted by the GNDVI model to be average. We sub-divided this field into three zones using the same model. We can see from this example that even though the overall predicted yield was for an average yield, further investigation reveals that there are both high and low yielding areas present in the field. A summary of the GNDVI values from the three areas are given in Table 2.

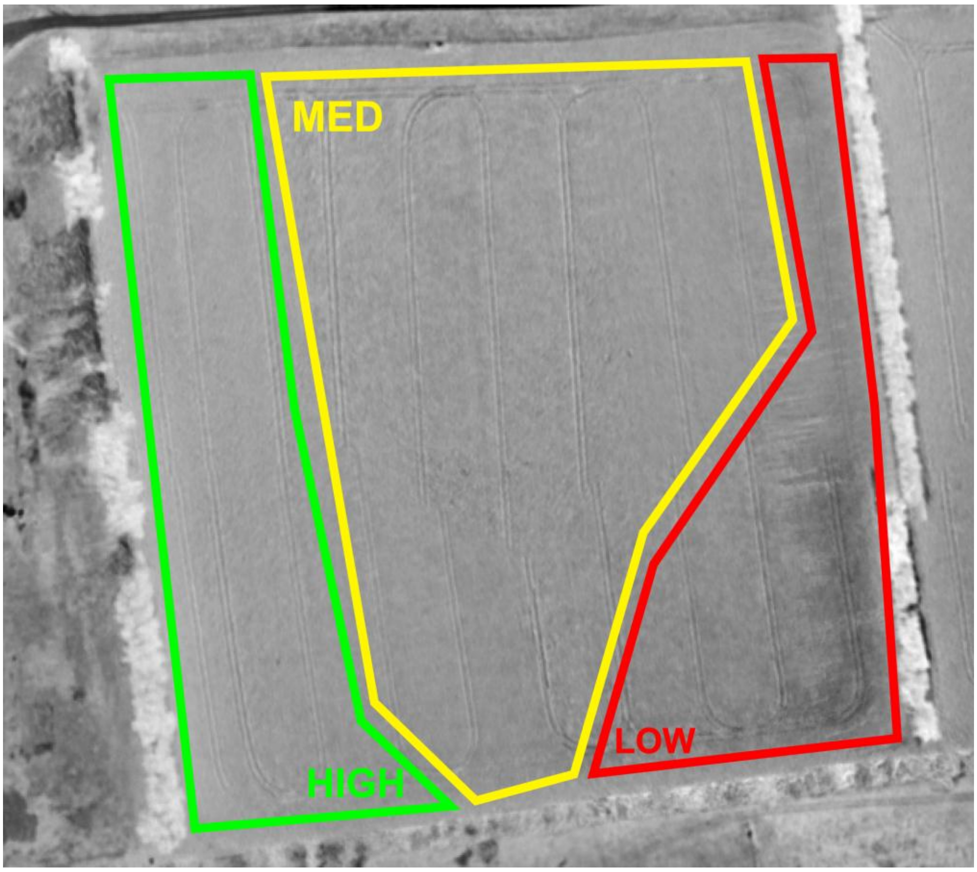

Figure 8: In this field we can define 3 different yield zones based on the average GNDVI score for that area.

Zone	GNDVI	% of total area
HIGH	0.65	22%
MED	0.61	53%
LOW	0.49	25%

Table 2: Yields and GNDVI scores from 14 fields

Notice that these intra-field differences are not easily distinguishable from the normal colour images and only become clear in the GNDVI images. For example, in Figure 9 both the GNDVI image and the normal colour image of a field are shown. Two low yielding areas have been highlighted on the GNDVI image and can also be identified as slightly darker than the surrounding field. However, these differences in colour do not show up on the normal colour image shown on the right.

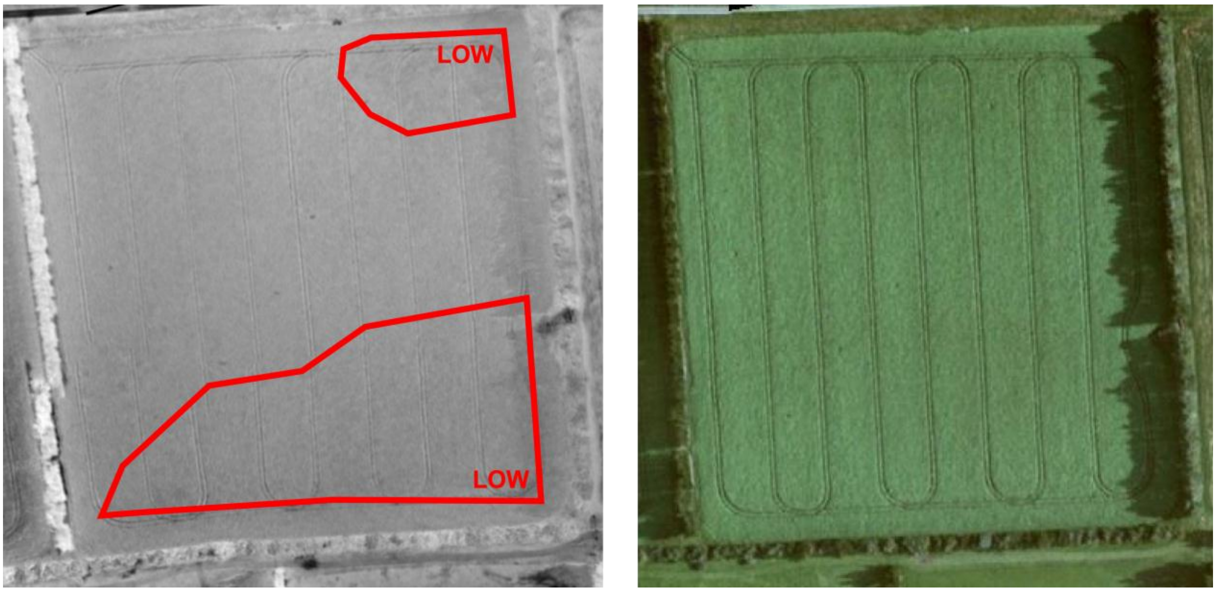

Figure 9: In the GNDVI image on the left the low yielding areas can be identified as darker parts of the field but these variations are not easily seen in the normal colour image of the same field on the right.

As we currently only have yield data on a per field basis it is not possible to verify these intra-field subdivisions based on the GNDVI. As future research we aim to collect yield data at a much higher spatial resolution so that this model can be further developed and verified.

Conclusions

The analysis of biomass yield (dry matter) from forage crops is difficult, especially when no mechanised harvesting process is possible, but grazing through livestock is conducted. Testing the possibilities linked with remote sensing data is a logical next step. The provision of such data becomes more practically feasible with unmanned aerial vehicles (UAV/ RPAS).

The good results presented here are somehow surprising, as other research often found poor correlation of remote sensing data with yield. One explanation may be linked to the GNDVI calculations that in this case are correlated to a full vegetative biomass, thus the ‘visible’ leaves and stems of this crop. The typical remote sensing work on yield estimation is related to cash crops where the targeted products are part of the biomass and not those directly being observed. The other explanation is found with the experimental design that studied whole fields (with sub-sections) and covered several fields as a larger block of fields. This allowed for more reliable modelling than with a traditional approach explaining yield variations exclusively within one individual field.

The error of assessing this dry matter yield with traditional, manual sampling of random or preselected 1m² subplots is high (20% to 30%). Improving this by ground work has limitations due to labour demand and high uncertainty of determining representative sites. The proposed method allows at least directing the manual sampling to areas that are identified as most likely of similar yield (classes). It is still necessary to determine the error of yield assessment with the remote sensing method.

Further investigations are necessary to identify the impact of annual (weather) variations as well as those impacts caused by diseases, high weed infestations as well as those from special soil conditions and varying nutrient management. It will also be necessary to study more varieties (with different stem to leaf ratio) as well as other species of forage crops.

Acknowledgment
This research is funded by an Agribusiness Innovation Grant of the Agricultural and Marketing Research and Development Trust in New Zealand and by contributions from SYNLAIT Farms in New Zealand.

References

Battiato, S., A. Castorina, and G Messina. *Single-Sensor Imaging: Methods and Applications for Digital Cameras.* London: CRC Press, 2008.

Gitelson, Anatoly, and Mark N. Merzlyak. "Spectral Reflectance Changes Associated with Autumn Senescence of Aesculus hippocastanum L. and Acer platanoides L. Leaves. Spectral Features and Relation to Chlorophyll Estimation." *Journal of Plant Physiology* 143, no. 3 (1994): 286-292.

Hoffmann, C. M., and M. Blomberg. "Estimation of Leaf Area Index of Beta vulgaris L. Based on Optical Remote Sensing Data." *Journal of Agronomy and Crop Science* 190, no. 3 (2004).

JAI. *JAI Multi-spectral Imaging.* JAI. 26 June 2014. http://www.jai.com/en/products/multi-imager/multi-spectralimaging (accessed June 24, 2014).

Judson, H. G., and G. R Edwards. "Survey of management practices of dairy cows grazing kale in Canterbury." *Proceedings of the New Zealand Grassland Association.* 2008. 249-254.

Matthew, C., N. J. Nelson, D. Ferguson, and Y. Xie. "Fodder beet revisited." *Agronomy New Zealand*, 2011: 39-48.

Moges, S. M., W. R. Raun, R. W. Mullen, K. W. Freeman, G. V. Johnson, and J. B. Solie. "Evaluation of Green, Red, and Near Infrared Bands for Predicting Winter Wheat Biomass, Nitrogen Uptake, and Final Grain Yield." *Journal of Plant Nutrition* 27, no. 8 (2005): 1431-1441.

Pangborn, M.C., and S.J. Gibbs. "Comparison of Winter Feeding Systems in Canterbury." online (http://maxa.maf.govt.nz/sff/about-projects/search/L09-028/), 2011.